CLM-P620

CLM-P620

UKAEA

Preprint

THE POWER BALANCE IN AN RFP REACTOR

J. P. CHRISTIANSEN
K. V. ROBERTS

CULHAM LABORATORY
Abingdon Oxfordshire

1980

CLM-P620

THE POWER BALANCE IN AN RFP REACTOR

J.P.Christiansen and K.V.Roberts
Culham Laboratory,Abingdon,Oxon,OX14 3DB,UK
(EURATOM/UKAEA Fusion Association)

ABSTRACT

A simplified power-balance equation is used to study the performance of a pulsed Reversed Field Pinch reactor, including the practicability of ignition by ohmic heating. Since only limited information about the energy confinement time τ_E is available from the RFP experiments carried out so far, which do not extend beyond 150 eV, we treat τ_E as an adjustable function in the model, and for the time being employ alternative empirical Tokamak scaling laws in the numerical estimates. The known heating rates and energy losses are represented by the net energy replacement time τ_W which is exhibited as a surface in density (n) and temperature (T) space with a saddle-point (n_*, T_*). Reactor performance estimates are made using a zero-dimensional power-balance model supplemented by calculations using the 1D ATHENE code. It is concluded that while ignition by ohmic heating is more practicable for the RFP reactor than for a Tokamak reactor with the same τ_E, the RFP energy confinement time would still require to be considerably better than that predicted by current Tokamak scaling laws to allow ohmic ignition in an RFP reactor with minor radius 1.75 m. If the minor radius could be reduced to (say) 1 m then ohmic ignition would be more practicable. More definitive estimates require a knowledge of τ_E which can only be obtained by extending RFP experiments closer to the reactor regime.

(submitted for publication in Nuclear Fusion)

Sept.1980

1. INTRODUCTION

This paper considers a pulsed fusion reactor system based on the Reversed Field Pinch (RFP) [1,2], with a cycle consisting of start-up, burn and shut-down phases [3] as in the conventional Tokamak. Although most of the studies of toroidal pulsed reactors [3-5] have been concerned with the Tokamak concept, the RFP could have engineering advantages: see for example the review articles by Bodin and co-workers [2,6], and the proceedings of the 1978 Padua Workshop [7,8]. One potential advantage is the use of higher β-values and lower toroidal magnetic fields in the RFP compared to the Tokamak, and another is the possibility of ignition by ohmic heating alone, instead of by the combination of ohmic and auxiliary heating that is required in the majority of Tokamak designs. It should however be stressed that whether or not these advantages can be realised in practice depends on quantitative factors that are not yet well understood due to a lack of experiments in the relevant parameter ranges: for example the influence of anomalous thermal transport on the energy confinement times, and the effect of the g-mode on the maximum β that can be achieved [9].

The review by Bodin and Newton [2] explains the main line of RFP research up to 1979 and how the RFP differs from the Tokamak. The potential advantages of the RFP reactor concept were identified quite early [10] and have since then been included in the further assessments of RFP reactor designs [11,12]. More recently a collaborative study [13] of a pulsed RFP reactor has led to a conceptual reactor design [13,14] based on this configuration. The choice of parameters made in [13,14]is dictated by economic and engineering constraints which impose a set of restrictions on the reactor plasma. Fixed plasma parameters are used to meet the design performance level (e.g., density, operating temperature, burn time etc.), and the physics assumptions also include plasma stability and ignition by ohmic heating. The RFP reactor design [14] has been updated [15],and reference [16]outlines a similar RFP reactor design together with other designs based on alternate concepts.

The object of this paper is to investigate these physics assumptions. We study the power balance of an ohmically-heated plasma, mainly from the viewpoint of the RFP reactor although much of the discussion would also apply to the Z-pinch and to the ohmically-heated Tokamak reactor. Our intention is to estimate the plasma parameters (density and temperature)

and reactor parameters (minor and major radii, toroidal current) that are required to achieve a given performance (power output, duty cycle, wall load, pulse length etc).

Our study starts from a simplified zero-dimensional power balance model. The various contributions to the power balance are outlined in §2 where the analytic expressions used for terms like ohmic heating etc. are given. The main problem in a study of this kind is that the energy confinement time τ_E is virtually unknown in the RFP reactor regime since experimental temperatures have not so far exceeded 150eV. For this reason it has been conventional [17] in RFP calculations to assume a Tokamak scaling law although even this involves considerable uncertainty in the extrapolation to reactor conditions [18]. As a practical step in the analysis, therefore, we separate in §3 the known power rates from the unknown energy losses due to thermal transport, impurity line radiation etc. The known power rates define a quantity called the net energy replacement time τ_W, and temperature equilibrium occurs when $\tau_E = \tau_W$.

The net energy replacement time τ_W (which also includes the known energy loss due to bremsstrahlung) depends on density n, temperature T, effective atomic number Z_{eff} and current density J, and we determine analytically the function $\tau_W(n,T,Z_{eff},J)$. At fixed Z_{eff}, J we exhibit the surface $\tau_W(n,T)$ in density-temperature space by an isometric projection and by contours of constant τ_W in the (n,T)-plane; examples of these representations are shown in Figs.1 and 2. The surface $\tau_W(n,T)$ always has a saddle-point $\tau_{W*}(n_*,T_*)$, where T_*= 7.4 keV is independent of J and of the resistivity anomaly factor. Saddle-point values are subscripted by an asterisk.

To calculate the energy growth time $\tau_G=(\tau_W^{-1}-\tau_E^{-1})^{-1}$, which is needed to study the evolution of the plasma to its burn regime, we need to specify the energy containment time τ_E. Various expressions (scaling laws) given in §2 are used in an attempt to bracket τ_G, and §4 shows two examples of how the surface $\tau_W(n,T)$ is deformed into a surface $\tau_G(n,T)$ by the choice of a specific scaling law for τ_E. The conditions for ignition by ohmic heating alone are analysed in §5 where all the τ_E scalings of §2 are applied; these conditions are expressed as limits on the reactor parameters minor and major radii and current. Although our results can only be tentative at present, it is expected that the method of analysis will remain useful when better experimental information on the RFP energy confinement scaling becomes available.

The reactor cycle is divided into three parts:

t_x, the time taken to establish the RFP configuration plus that needed for rundown and plasma exhaust; this is regarded as fixed in our study and its value is assumed to be 1 second.

t_*, the time taken to reach ignition; this will be shown to be the time taken to reach the saddle-point (n_*, T_*) of the surface $\tau_W(n,T)$ starting from some point $(n_o, T \approx 0)$.

t_b, the duration of a controlled thermonuclear burn at the operating point (n_1, T_1).

In §6 we show that t_*/τ_{E*} is a function only of the product $J\tau_{E*}$, where τ_{E*} is the value of τ_E at the saddle-point (n_*, T_*) irrespective of the scaling law used for τ_E. The burn time t_b is determined both by the reactor power output and by the duty cycle.

The results of §§ 3-6 are then applied to two reactor designs. §7 shows that the original design [13] requires an energy confinement time τ_{E*} which is several times the value predicted by some of the empirical Tokamak scaling laws. An alternative design with a smaller minor radius, but the same toroidal current allows τ_{E*} to be smaller than the values predicted by empirical Tokamak scaling laws. These two results are confirmed by detailed one-dimensional equilibrium-transport calculations with the ATHENE 1 code [19].

The performance of an RFP reactor depends strongly on anomalous losses, i.e., on the scaling of τ_E, for which little empirical information from RFP experiments is available. The study made in this paper has therefore made extensive use of empirical Tokamak scaling laws in order to compare the RFP with the Tokamak. The results show that a small minor radius (a $\sim$ 1m) RFP reactor can operate with an energy containment time which is less than the value required for the equivalent Tokamak reactor which, in addition, needs an auxiliary heating source to compensate for the smaller Ohmic input rate.

SI units are used with temperature expressed in either eV or keV.

2. The Power Balance Equation

To examine the conditions for thermonuclear ignition we start from a power balance equation written in the symbolic form

$$\frac{dW}{dt} = T + O - R - U + S \quad . \tag{1}$$

W is the total plasma energy density and the symbols on the RHS' denote

power density rates of Thermonuclear fusion, Ohmic heating, known Radiation losses, Unknown losses, and Sources of additional heating. Several papers have described ignition conditions in Tokamaks [20] and the particular roles of additional heating by neutral injection [21], by RF-heating [22] and by major radius compression [23]have also been investigated. For an RFP reactor no sources of additional heating are currently envisaged so that S = 0 is used in (1). The expressions for the remaining terms are simplified as follows:-

2.1. Plasma Energy Density

The plasma consists in general electrons and various ion species, and this is taken into account in the one-dimensional calculations. At present we assume a plasma of electrons and a 50-50 DT mixture plus a simplified impurity concentration level f such that $Z = 1 + fZ_o$, $Z_{eff} = (1+fZ_o^2)/Z$, where $Z_o = 8$ is used corresponding to fully ionized Oxygen. Ions and electrons share the same temperature T and the plasma energy density is

$$W = \frac{3}{2} n\ (1+Z)\ eT. \tag{2}$$

2.2. Thermonuclear heating rate

The rate of α-energy production from the D-T reaction is

$$T = \tfrac{1}{4} n^2 \langle\sigma v\rangle E_{DT}\ , \tag{3}$$

where for the cross section we use [24]

$$\langle\sigma v\rangle = 9\ 10^{-22} \exp\left(-0.476 \left|\ell n \frac{T}{6.9\ 10^4}\right|^{2.25}\right) \quad \left[m^3 sec^{-1}\right]. \tag{4}$$

The energy $E_{DT} = 5.6\ 10^{-13}$ J is to be deposited over some region of the RFP discharge. Many papers, e.g.[25,26], have studied the slowing down of α-particles in magnetic confinement systems, mainly Tokamak reactor configurations; these papers also study additional effects from α-particles, e.g. thermal stability properties. The major part of the α-energy is given to the electrons until the α-energy reaches a few hundred keV. During this slowing down period the α-particle drift orbit is not significantly perturbed by collisions. The spatial extent Δ_α over which α-energy is attributed to electrons is thus dependent only on the plasma equilibrium for an isotropic birth-velocity distribution. To estimate Δ_α it is necessary to track α-particle drift orbits numerically in various RFP equilibria; details of this will be given elsewhere. It is here sufficient to use (3) as a simple approximation.

2.3. Ohmic heating rate

With the Spitzer expression for the resistivity [27] the Ohmic heating rate becomes

$$O = c_O T^{-3/2}, \quad c_O = 5.22.\,10^{-5} J^2 c_a \ell n\Lambda, \tag{5}$$

where c_a is some anomaly factor which may depend on Z_{eff}.

2.4 Radiation losses

In general bremsstrahlung, recombination, line and synchrotron emission may contribute to the loss of energy by radiation. The last contribution will be negligible for an RFP reactor, while impurity radiation will depend on the types of impurities and on their relative concentration levels. Since these are not known we combine impurity radiation losses with the other unknown losses represented in τ_E, and assume that the term R in (1) just represents the bremsstrahlung rate

$$R = c_R n^2 T^{\frac{1}{2}}, \quad c_R = Z_{eff} Z^2 1.56\ 10^{-38}. \tag{6}$$

2.5. Unknown losses. Confinement times

Unknown losses include thermal losses by anomalous transport and impurity radiation. The term U of (1) is written as

$$U = W/\tau_E \tag{7}$$

where the energy containment time can be cast in several forms. The following 5 expressions are considered and superscripted c for classical [27], B for Bohm [27], HS for Hugill-Sheffield empirical scaling [28] A for Alcator scaling [29-30], PW for Pfeiffer-Waltz scaling [31]:

$$\tau_E^c = \frac{a^2 B^2 T^{\frac{1}{2}} 3 \varepsilon_o^2 e^{\frac{1}{2}} (2\pi)^{3/2}}{e^2 n m^{\frac{1}{2}} \ell n\Lambda M^{\frac{1}{2}}}, \tag{8a}$$

$$\tau_E^B = \frac{a^2 16 e B}{eT}, \tag{8b}$$

$$\tau_E^{HS} = x_1 n^{x2} I^{x3} R_o^{x4} M^{x5} a^{x6}, \tag{8c}$$

$$\tau_E^{Al} = 3.8\ 10^{-21} n a^2, \tag{8d}$$

$$\tau_E^{A2} = 8\ 10^{-24} n a^2 T \frac{a}{R_o} \frac{1}{B_p}, \tag{8e}$$

$$\tau_E^{PW} = 9.5\ 10^{-20} n^{0.9} a^{0.98} R^{1.63}. \tag{8f}$$

In the expressions (8) the symbols have their usual meaning and table I lists 3 sets of values for the empirically determined constants $x_1 - x_6$ obtained by Sheffield [28] from an adaptation of the Hugill-Sheffield scaling law. In many of the reactor studies [3-5, 20, 21, 25] various assumptions such as (8) are made for the τ_E scaling laws. At present we lack empirical information about anomalous losses in RFP geometry and the choices (8c-8f) reflect the assumption that the Ohmic heating phase of a large RFP should resemble that of a large Tokamak. (In the one-dimensional transport calculations various combinations of the expressions (8) are used in different parts of the discharge following the RFP model of [17]).

3. The net energy replacement time

The net energy replacement time τ_W is defined from (1) as

$$\frac{1}{\tau_W} = \frac{T + O - R}{W} \quad , \tag{9}$$

while the energy growth time is (see also [31])

$$\frac{1}{\tau_G} = \frac{1}{W}\frac{dW}{dt} = \frac{1}{\tau_W} - \frac{1}{\tau_E} \quad . \tag{10}$$

We have found it instructive to study the expression (9), since it does not contain the unknown losses. By inserting the expressions (2-6) in (9) we can write (9) as

$$\tau_W = \frac{nT}{A\,n^2 + C} \quad ,$$

or

$$A\,n^2 - Bn + C = O \quad . \tag{11}$$

The coefficients A,B,C are

$$A\,(T, Z_{eff}, Z) = \frac{T - R}{e\,n^2}\,\frac{2}{3(1+Z)}$$

$$B\,(T) = \frac{T}{\tau_W}$$

$$C\,(T, Z_{eff}, Z, J) = \frac{O}{e}\,\frac{2}{3(1+Z)}$$

For fixed J, Z and Z_{eff} we can plot contours of constant τ_W in the (n,T)-plane from the solutions to (11)

$$n_{+,-} = \frac{1}{2A}(B \pm D^{\frac{1}{2}}), \quad D = B^2 - 4AC.$$

Fig.1 shows an example of such a set of contours obtained for $Z = Z_{eff} = 1$ and $J = 7$ MA m^{-2}. The surface $\tau_W(n,T)$ is shown as an isometric projection in Fig.2 for the same values of Z, Z_{eff} and J. The surface $\tau_W(n,T)$ always has a saddle-point $\tau_{W*}(n_*,T_*)$ as can be seen from Figs.1 and 2 and the location of this saddle-point is found from the two extremum curves

$$\frac{\partial \tau_W}{\partial n} = 0, \quad n_n^2(T) = \frac{C}{A}, \quad \tau_{Wn} = T(4AC)^{-\frac{1}{2}}, \tag{12}$$

$$\frac{\partial \tau_W}{\partial T} = 0, \quad n_T^2(T) = \frac{T\,C' - C}{A - T\,A'}, \quad \tau_{WT} = \frac{n_T T}{A\,n_T^2 + C}, \tag{13}$$

the prime denoting $\frac{\partial}{\partial T}$. The curves $n_n(T)$ and $n_T(T)$ intersect when

$$T \frac{\partial}{\partial T} \ell n\,(AC) = 2,$$

so that the value T_* is independent of J and any resistivity anomaly factor c_a in (5). The saddle-point co-ordinates can be calculated as functions of Z_{eff} and the result is

$$\begin{aligned} T_* &= s_T(Z_{eff})\ 7.41 && [\text{keV}] \\ n_* &= s_n(Z_{eff})\ 1.62\ 10^{13}\ J && [m^{-3}] \\ \tau_{W*} &= s_\tau(Z_{eff})\ 1.96\ 10^{7}\ \frac{1}{J} && [s] \end{aligned} \tag{14}$$

The s functions are plotted in Fig.3 against Z_{eff} in the range $Z_{eff} = 1$ to $Z_{eff} = 2$. It can be seen that T_* increases with Z_{eff} while n_* and τ_{W*} decrease slightly.

From (14) we can calculate two quantities of interest. The drift parameter (drift speed divided by electron thermal velocity) is

$$\xi_* = \frac{J}{Zen_* v_{e*}} = 1.05\ 10^{-2}\ \frac{1}{Z\,s_T^{\frac{1}{2}} s_n} \approx 1\%$$

and the rate of power input to the plasma is

$$P_* = \frac{W_*}{\tau_{W*}} = 1.48\ 10^{-9}\ J^2\ (1+Z)\ \frac{s_n s_T}{s_\tau} \qquad [W] \ .$$

4. The energy growth time

To calculate the energy growth time (eq. 10) we need to know the energy containment time. Guided by the scaling laws (8) for τ_E we set

$$\tau_E = \tau_{E_*} \left(\frac{n}{n_*}\right)^{u1} \left(\frac{T}{T_*}\right)^{u2} \ , \qquad (15)$$

where subscript * refers to the saddle-point values. The unknown exponents u1 and u2 can be assigned values according to the choice of scaling law, but following (8) we assume

$$-1 \le u1 \le 1 \ , \qquad -1 \le u2 \le 1 \ . \qquad (16)$$

The saddle-point value τ_{E*} in (15) may depend on J (or B), a, R_o, Z_{eff} etc. If we insert the expressions (14-15) in (10) we obtain

$$\tau_G = \tau_{E*}\ G(n,\ T,\ J\ \tau_{E*},\ Z_{eff}) \qquad (17)$$

for a given set of values u_1, u_2. Thus for any τ_E scaling law the energy growth time is a function only of n,T and the product $J\tau_{E*}$ (and Z_{eff}). We can therefore represent τ_G as a surface $\tau_G(n,T)$ for every value of J and study how the surface $\tau_W(n,t)$ is deformed to $\tau_G(n,T)$ by the choice (15). Two examples of $\tau_G(n,T)$ are shown in Figs.4 and 5. Both curves have $J = 7\ MAm^{-2}$, as for Fig.1 and 2, and Fig.4 corresponds to $u_1 = 1$, $u_2 = 0$ (Alcator scaling) while Fig.5 corresponds to $u_1 = 0$, $u_2 = -1$ (Bohm scaling). The values of τ_{E*} in Figs.4 and 5 are chosen larger than τ_{W*} given by (14), so that τ_{G*} is positive. The analysis in § 3 of the surface $\tau_W(n,T)$ can naturally be extended to the surface $\tau_G(n,T)$ for every choice of τ_E.

5. Ignition conditions

The condition for ignition by Ohmic heating alone is that the energy growth time τ_G is positive. This will be the case for any density (see eq.13)

$$n = n_T < \left(-\frac{C}{A}\right)^{\frac{1}{2}}$$

provided that

$$\tau_E\ (n_T) > \tau_{WT}\ (n_T) \quad ,$$

where the above quantities are given in § 3. The smallest value of τ_{WT} (eq.13) occurs at the saddle-point, so that the ignition condition becomes

$$\tau_{E*} > \tau_{W*} \tag{18}$$

(A different value of τ_E may be required at the true saddle-point τ_{G*} of the τ_G surface; the position of this point is however now known unless τ_E is known which is why (18) applies at the saddle-point τ_{W*}). In order to examine whether (18) can be satisfied by the scaling laws (8) we set

$$\tau_{E*} = \varepsilon_j\ \tau_{E*}^j$$

where j stands for classical, Bohm, Hugill-Sheffield, Alcator scaling, Pfeiffer-Waltz scaling and ε_j is an anomaly factor. The magnetic field configuration we choose is a Bessel function model [32] for which B and J on axis are related to the current I and to the minor radius a via

$$\begin{aligned} B &= \frac{\mu_o\ I}{2\pi a\ J_1(\theta)} \quad \doteq \quad 4.76\ 10^{-7}\ \frac{I}{a}\ [T]\ , \\ J &= \frac{I\ \theta}{\pi a^2\ J_1(\theta)} \quad = \quad 1.06\ \frac{I}{a^2}\ [Am^{-2}]\ . \end{aligned} \tag{19}$$

A pinch parameter $\theta = 1.4$ has been assumed. The ignition condition (18) can then be written as

$$a^{u3}\ R_o^{u4}\ \varepsilon_j^{u5}\ I > U_j \tag{20}$$

for all scaling laws; Table II gives the values of the exponents u3-u5 and the constants U_j for all the scaling laws (8) for the case $Z_{eff} = 1$. The ignition condition (18) can also be cast in other forms the best known [33] being obtained from (14) as

$$n_*\tau_{E*} > 3.2\ 10^{20} s_n s_\tau [m^{-3}s] \quad \text{or} \quad J\tau_{E*} > 1.96\ 10^7 s_\tau [Am^{-2}s] \tag{21}$$

If a fixed current I is assumed then all scaling laws except the classical law result in

$$a < \varepsilon^{u6}\ a_{max}\ .$$

Table II also gives the values of a_{max} for I = 20 MA, R_o/a = 10, and τ_{E*} for two values of a. It can be seen that the empirical scaling laws (8c - 8f) predict a_{max} to within a factor of appr. 15 and τ_{E*} to within a factor 25. This means that to achieve ignition (21) there is a large uncertainty factor in the required ohmic input rate J^2. Hence if a reactor plasma is assisted by additional heating (Tokamak) to overcome the 'thermal inertia' in the saddle-point region this large uncertainty factor would apply to the power level of additional heating.

6. The reactor cycle

We mentioned earlier that one cycle of a pulsed reactor is divided into three parts and here we consider the duration t_* of the approach to the saddle-point and the burn period t_b. The time t_* taken to reach the saddle-point (n_*, T_*) starting from some initial point $(n_o, T \approx 0)$ is found by integrating (17) as

$$\frac{t_*}{\tau_{E*}} = \int_o^{W_*} G(W, n, J\,\tau_{E*}, Z_{eff})\; d(\ell n\; W) \qquad (22)$$

where $W = \frac{3}{2}\, n(1+Z)eT$ is the plasma energy density. The ratio t_*/τ_{E*} depends only on $J\tau_{E*}$ (and Z_{eff}) and the path $n = n(W)$ in the (n, W) plane connecting the starting point to the saddle-point. The Euler equation describing that path which minimizes the integral (22) is simply

$$\frac{\partial G}{\partial n} = 0$$

because we have only specified $\frac{dW}{dt}$ (eq. 1). One "optimum" path thus consists of an isochor (heating at constant n_o) together with an isotherm (gas puffing at $T = T_*$ if $n_o \neq n_*$). The integral (22) can be evaluated for various values of the unknown exponents ul and u2 in (15) within the window (16) for various paths, e.g. path of constant ξ, adiabatic path etc. Fig.6 shows 3 curves representing the ratio t_*/τ_{E*} vs. $J\tau_{E*}$. The solid curve represents heating at n_* for any (u_1, u_2) satisfying (16); the dashed curve corresponds to $n_o = 0.1\, n_*$ and $u_1 = 1$, $0 \leq u_2 \leq 1$; the dotted-dashed curve also has $n_o = 0.1\, n_*$, but $u_1 = 0$. From Fig.6 we see that for large $J\tau_{E*}$, the time t_* is almost independent of τ_{E*}. However near the marginal ignition condition (21) any large uncertainty factor in τ_{E*} only leads to an uncertainty factor of appr. 10 in t_*.

Once the saddle-point has been reached the plasma can be made to move rapidly to a burn regime (n_1, T_1). Various additional energy loss mechanisms required to achieve a stable burn can be envisaged, but such mechanisms will not be dealt with here.

The burn time can be determined from the requirement that the total reactor power output (α-heating + neutrons) averaged over one cycle should be $P_R = \bar{P}V$, where V is the reactor volume ($V = 2\pi^2 a^2 R_o$ for a circular cross section torus). The axial power density is related to the space-time averaged value by $\bar{P} = P\,\lambda/\zeta$, where λ, typically of order 0.3, depends on density-temperature profiles and where ζ, the duty cycle factor, is

$$\zeta = \frac{t_b}{t_x + t_* + t_b} = \frac{t_b}{t_o} \quad . \tag{23}$$

The burn time can therefore in principle be found from

$$t_b(n_1, T_1, P_R, V) = \frac{P_R\,\lambda\,(t_x + t_*)}{5V\mathcal{T} - P_R\lambda} \quad ,$$

the α-heating rate $\mathcal{T}$ being given by (3). More often it is necessary to impose a lower limit ζ_o on (23) and this determines $t_b = t_b(J\tau_{E*}, \zeta_o)$; n_1 and T_1 are then found from

$$P_R = 5\,\lambda\,\mathcal{T}(n_1, T_1)\,V/\xi_o \tag{24}$$

During the approach to the saddle-point and during the burn the reactor configuration has to remain grossly MHD-stable. It is difficult to derive a simple condition for stability, but in the one-dimensional equilibrium-transport calculations the slowly decaying RFP configuration is tested against gross instability. In the absence of an internal plasma dynamo [34] an RFP configuration decays resistively [6,17,34,35] on a timescale τ_c which clearly has to exceed $t_* + t_b$. Stability against excess pressure means that the plasma β cannot exceed a certain value β_{max} which can be estimated from the diagram in ref.[35] relating the axial β to the pinch parameter. Using (19) we thus enforce

$$\beta = \frac{n(1+Z)eT}{B^2/2\mu_o} = 1.78\ 10^{-12}\ n_1 T_1 \left(\frac{a}{I}\right)^2 (1+Z) \le \beta_{max} \tag{25}$$

and typically $\beta_{max} = 0.2 - 0.25$ for the pressure inflated Bessel-function model [17,35].

The thermal flux plus neutron flux on the wall is regarded as a fixed quantity; the wall load given by

$$F_w = \frac{P_R}{4\pi^2 a R_o} \tag{26}$$

is small initially and rises to its peak value during burn.

For a given reactor performance F_w, P_R, ζ_o and t_o we see that (21-26) relate the 4 performance figures to the reactor parameters a, R_o, I and the plasma parameters n_1, T_1. For an RFP reactor we are free to choose a and R_o independently (unlike a Tokamak) as long as (26) is satisfied. From (24) and (26) we derive for fixed T_1 the following scaling with minor radius a: density $n_1 \sim a^{-\frac{1}{2}}$, line density $N = n_1 a^2 \sim a^{3/2}$, power per unit length $P_R/R_o \sim a$, plasma beta $\beta \sim a^{3/2}$.

7. Reactor parameters

In reactor design it is customary to start from a given set of values of wall load F_w, power output P_R, duty cycle ζ_o and pulse period t_o, since these parameters are determined principally by engineering constraints. Table III gives the values used and the relations (23) and (26) then imply

$$t_* = 4[s], \quad aR_o = \frac{250}{\pi^2}\,[m^2], \quad V = 500a[m^3].$$

The ignition conditions (20) for the scaling laws then become $I > I(a)$. Fig.7 shows the required current against minor radius with anomaly factors $\varepsilon = 1$ for the empirical scaling laws (8c-8f) and $\varepsilon_{class} = 10^{-2}$, $\varepsilon_{BOHM} = 100$ chosen to keep the diagram compact. The minimum value $\tau_{E*} = \tau_{W*}$ of τ_E at the saddle-point required for ignition is shown against a in Fig.8 together with $\tau_{E*} = \tau_{E*}(a, I=20MA)$ for the scaling laws (8) using the same values of ε as in Fig.7. Although Fig.7 suggests a high value of I (50MA at a = 2m) to satisfy all scaling laws (8) we consider only I = 20MA which is the value assumed in the designs [13-16]. With this value of I we examine the ignition conditions (20) together with the relations (22-25) for two values of minor radius: 1) a = 1.75m[13] and 2) a = 1m. The corresponding values of I required for ignition are marked with circles and crosses in Fig.7.

One-dimensional equilibrium-transport calculations with the ATHENE 1 code [19] have been carried out for these two reactor designs. The model used in [19] is described in [17] and in addition we include α-heating, gas-puffing and an anomalous electron diffusivity related to the τ_E scaling law (8c,case 1). The α-particles remain on a flux surface until their energy reaches 300keV at which stage they are allowed to diffuse across the discharge. The gas-puffing assumes cold DT gas to be transported uniformly across the discharge and to mix with the host plasma on a short timescale.

The results are summarized in Table III which gives the values of all reactor parameters as well as the τ_{E*} value required to reach ignition in 4 seconds and the anomaly factor ε needed for (8c,case 1) to produce τ_{E*}.

The conclusions of our study are of course based on the scaling laws for the confinement time τ_E. The larger reactor with a = 1.75m requires of order 5-7 times the value of τ_E predicted by perhaps a pessimistic choice of τ_E scaling, while the smaller reactor with a = 1m requires a τ_E less than that value. This result provides however an insufficient basis for preferring a smaller reactor, since the actual τ_E scaling laws for an RFP reactor may be different from the Tokamak scaling laws (8). Indeed recent results from the Alcator C Tokamak experiment [36] show departures from the previously assumed scaling law (8d).

Scaling Law	X_1	X_2	X_3	X_4	X_5	X_6
1	0.0583	0.503	0.924	0	0	-0.198
2	0.0466	0.653	0.875	1.057	0	-0.423
3	0.0502	0.649	0.801	1.006	1.101	-0.310

TABLE I. Values of the constants used to calculate the expression (8c) are taken from [28]. n is in units of $10^{20}(m^{-3})$, I in (MA), R,a in (m).

Scaling Law	u3	u4	u5	U	a_{max}[m] I=20[MA]	τ_{E*}[s], a=1.75m	I=20[MA] a = 1m
Class(8a)	0	0	0.5	0.58	-	3438	1120
Bohm(8b)	-0.5	0	0.5	135	0.022	0.036	0.02
H-S1(8c)	-1.43	0	0.45	19.3	1.02	0.88	1.73
H-S2(8c)	-1.05	0.42	0.4	16.9	2.95	10.2	48.5
H-S3(8c)	-1.06	0.41	0.4	11.8	4.0	20.5	87.3
Alc.1(8d)	-1	0	0.5	16.8	1.2	1.3	1.3
Alc.2(8e)	0	-1	1	3.64	0.55	1.07	0.2
P.W (8f)	-1.48	0.85	0.53	36.9	8.3	17.8	53.0

TABLE II. Parameter values in the expression (20)
$a^{u3} R_o^{u4} \varepsilon^{u5} I > U$
for the scaling laws (8). For I = 20[MA] and R_o=10a this leads to the values a_{max}. The saddle-point values τ_{E*} predicted by (8) are given for I = 20MA and (a,R_o) = (1.75,16.5) and (1,25.3) respectively.

Plasma Reactor parameters	a = 1.75m	a = 1m
Major radius R_o [m]	16.5	25.3
Volume V [m^3]	1000	500
Wall area [m^2]	1000	1000
Power output P_R [GW]	2	2
Wall load F_w [MWm^{-2}]	2	2
Duty cycle ζ_o	0.9	0.9
Pulse length t_o [s]	50	50
Current I [MA]	20	20
Current density J [MAm^{-2}]	7	20
Toroidal Field B [T]	5.5	9.5
Plasma density n_l [$10^{20} m^{-3}$]	3	4
Line density N [$10^{20} m^{-1}$]	20	9
Temperature T_l [keV]	20	20
Beta β [%]	16	7
Ignition time t_* [s]	4	4
Required value of τ_{E*} [s]	4	1
Anomaly factor ε	5	0.6

TABLE III. Comparison between reactor parameters for 2 values of minor radius a.

REFERENCES

[1] BODIN, H.A.B., KEEN, B.E. Rep.Prog.Phys. 12, (1977) 1415.

[2] BODIN, H.A.B., NEWTON, A.A., Nucl.Fusion (in the press)

[3] INTOR Group, 'International Tokamak Reactor', Nucl.Fusion 20, 1980) 349;
INTOR International Tokamak Reactor, Zero Phase, IAEA Vienna (1980).

[4] For early work see: CARRUTHERS, R., DAVENPORT, P.A., MITCHELL, J.T.D., 'The Economic Generation of Power from Thermonuclear Fusion', Culham Laboratory Report CLM-R85(1967); ROSE, D.J., 'On the Feasibility of Power by Nuclear Fusion', Oak Ridge National Laboratory Report ORNL-TM-2204 (1968); articles in Proceedings of the BNES Nuclear Fusion Reactors Conference, Culham Laboratory, September 1969; articles in International School of Fusion Reactor Technology 'Pulsed Fusion Reactors', Erice-Trapani(Sicily) Sept.1974, Pergamon Press, Oxford (1975).

[5] For recent work and references see articles in: Fusion Technology 1978, Vols.1 and 2, published for the Commission of the European Communities by Pergamon Press, Oxford (1979).

[6] BODIN, H.A.B., Third Topical Conference on Pulsed High Beta Plasmas, (ed.D.E.Evans), P.39, Pergamon Press, Oxford (1976).

[7] ORTOLANI, S., Reversed-Field Pinch (RFP) Configuration, Report on the International Workshop held at Padua, September 1978, Nucl.Fusion 19, (1979) 535.

[8] Proceedings of the Workshop on the Reversed Field Pinch (RFP), Universita di Padova, Instituto di Elettrotecnica e di Elettronica, Report UPee 78/08, September 1978.

[9] CAROLAN, P.G., GOWERS, C.W., ROBINSON, D.C., WATTS, M.R.C., BODIN, H.A.B. 7th International Conference on Plasma Physics and Controlled Nuclear Fusion Research 1978, paper IAEA-CN-37/E-1-2, IAEA, Vienna(1979).

[10] BODIN, H.A.B., JAMES, T.E., NEWTON, A.A., 'A Pulsed Fusion Reactor based on the Toroidal Pinch', BNES Nuclear Fusion Reactors Conference, Culham Laboratory, September 1969, p.255.

[11] BAKER, D.A., DIMARCO, J.A., FORMAN, P.R., PHILLIPS, J.A., Los Alamos Report LA-UR-2338 (1975); HAGENSON, R.L., Los Alamos Report LA-UR-2190 (1976).

[12] BODIN, H.A.B., BUTT, E.P., CARRUTHERS, R., JAMES, T.E., NEWTON, A.A., ROSTAGNI, G., in Plasma Physics and Controlled Fusion Research (Proc.5th Int.Conf.Tokyo, 1974) 3, IAEA, Vienna (1975) 631.

[13] LAWSON, J.D., Reversed Field Pinch Reactor Study, I, Physical Principles, Culham Report CLM-R171 (1977).

[14] HANCOX, R., SPEARS, W.R., Reversed Field Pinch Reactor Study II, Choice of parameters, Culham Report CLM-R172 (1977);
HOLLIS, A.A., MITCHELL, J.T.D., Reversed Field Pinch Reactor Study III, Preliminary Engineering Design, Culham Report CLM-R173 (1977).

[15] HANCOX, R., et al: in Fusion Reactor Design Concepts (Proc. Tech Committee Meeting and Workshop, Madison,1977) IAEA Vienna (1978) 319.

[16] BATHKE, C.G.,et al: Paper IAEA-CN-38/VA, 8th Int.Conf. on Plasma Physics and Controlled Nuclear Fusion Research, Brussels,1980.

[17] CHRISTIANSEN, J.P., ROBERTS, K.V., Nucl.Fusion 18 (1978) 181.

[18] CORDEY, J.G., 8th Int.Conf. on Plasma Physics and Controlled Nuclear Fusion Research, Brussels 1980, Magnetic Confinement Theory Summary Paper.

[19] CHRISTIANSEN, J.P., ROBERTS, K.V., LONG,J.W., Comp.Phys.Comm. 14,(1978) 423.

[20] GIBSON, A., Proc. BNES Conf.on Nuclear Fusion Reactors (Culham 1969) 194.
MILLS, R.G., Nuclear Fusion 7 (1967) 223.
BROMBERG, L., COHN, D.R., FISHER, J.L., Nucl.Fusion 19,(1979) 1359.
HARVEY, R.W., RAWLS, J.M., Nucl.Fusion 19,(1979) 869.

[21] SWEETMAN, D.R., Nuclear Fusion 13 (1973) 157.

[22] FURTH, H.P., Tokamak Research in the US, 9th European Conf.on Controlled Fusion and Plasma Physics, Oxford (1979).

[23] BORASS, K., LACKNER,K., MINARDI,E., 9th European Conf. on Controlled Fusion and Plasma Physics, Oxford (1979) Paper DP16.

[24] BRUNELLI, B., An Empirical formula for the DT reactivity with applications to fusion reactor dynamics, Frascati Report, Frascati 1978.

[25] KOLESNICHENKO, Ya,I., REZNIK,S.N., YAVORSKIJ, V.A., Nucl.Fusion 16 (1976) 105.

[26] SAITO, H., SEKIGUCHI, T., KATSURAI, M., MAEKAWA, S., Nucl.Fusion 17, (1978) 919.
OHNISHI, M A.O., WAKABAYASHI, J., Nucl.Fusion 18, (859).
SIGMAR, D.J., CHAN, H.C., Nucl.Fusion 18,(1978) 1569.

[27] SPITZER, L., Physics of fully ionized gases, Interscience Publishers, New York (1965).

[28] HUGILL, J., SHEFFIELD, J., Nucl.Fusion 18,(1978) 15;
SHEFFIELD, J., Private Communication, Jan.1977.

[29] DAUGNEY, C.C., Nucl.Fusion 15, (1975) 967.

[30] MURAKAMI, M., EUBANK,H.P., Physics Today, May 1979, pp 25-32.
MAZZUCATO, ., COPPI, B. Phys. Letters 71A(1979) 337.
[31] PFEIFFER,W., WALTZ, R.E., Nucl.Fusion 19,(1979) 51.

[32] TAYLOR, J.B., Phys.Rev.Lett.33 (1974) 1139.

[33] LAWSON,J.D., Proc.Phys.Soc.70 (1957) 6.

[34] GIMBLETT,C.G., WATKINS, M.L., Pulsed High Beta Plasmas, Pergamon Press,(1976) 279.

[35] GOWERS,C.W. et al. in Plasma Physics and Controlled Fusion Research (Proc.6th Int.Conf.Berchtesgaden 1976) 1, IAEA Vienna,(1977) 429.

[36] PARKER, R.R., and Alcator Group, Paper IAEA-CN-38/N6, 8th Int.Conf.on Plasma Physics and Controlled Fusion Research, Brussels, 1980.

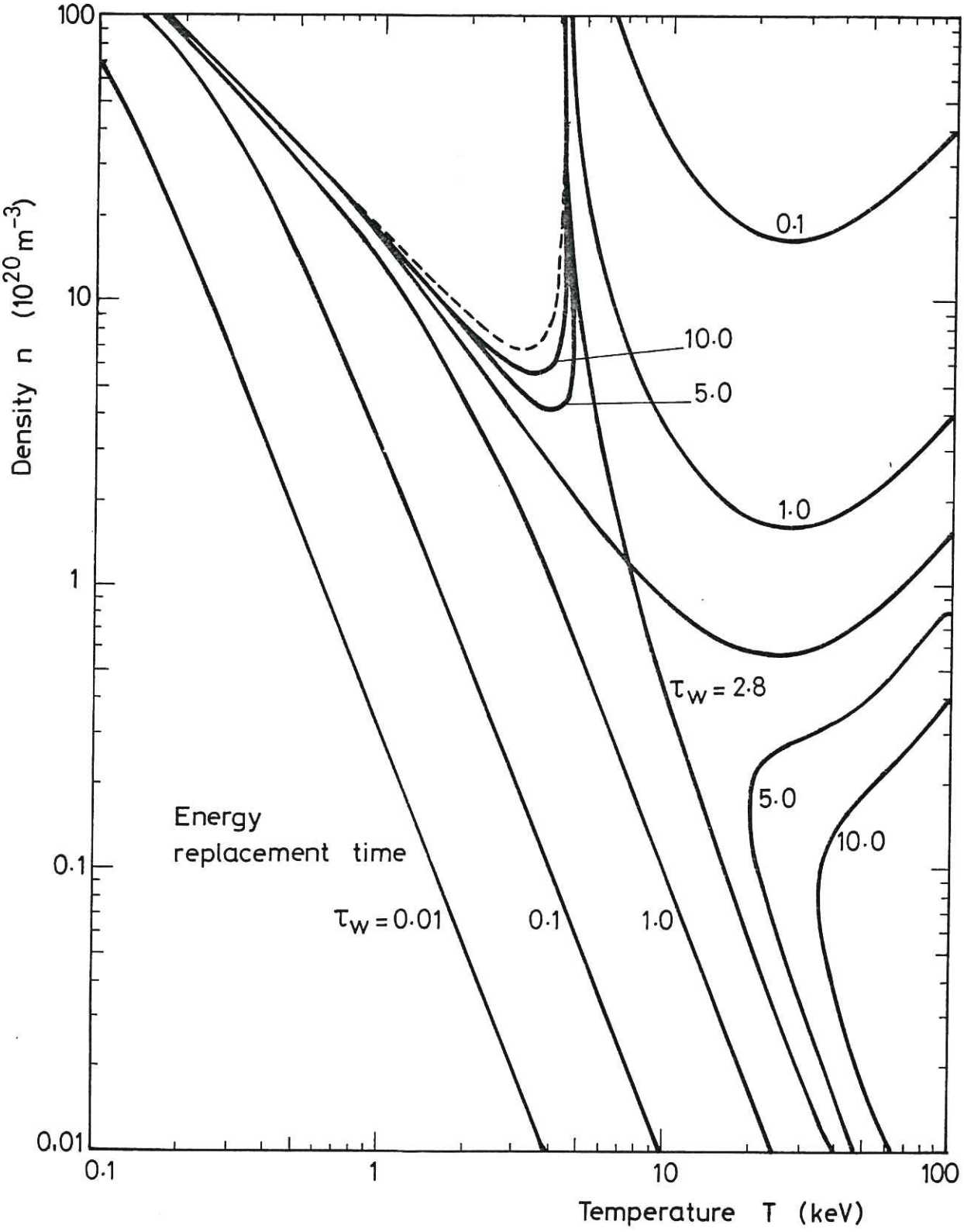

Fig.1 Contours in the (n,T) plane of constant τ_W the energy replacement time defined by (9). J = 7 [MAm^{-2}] and Z_{eff} = 1.

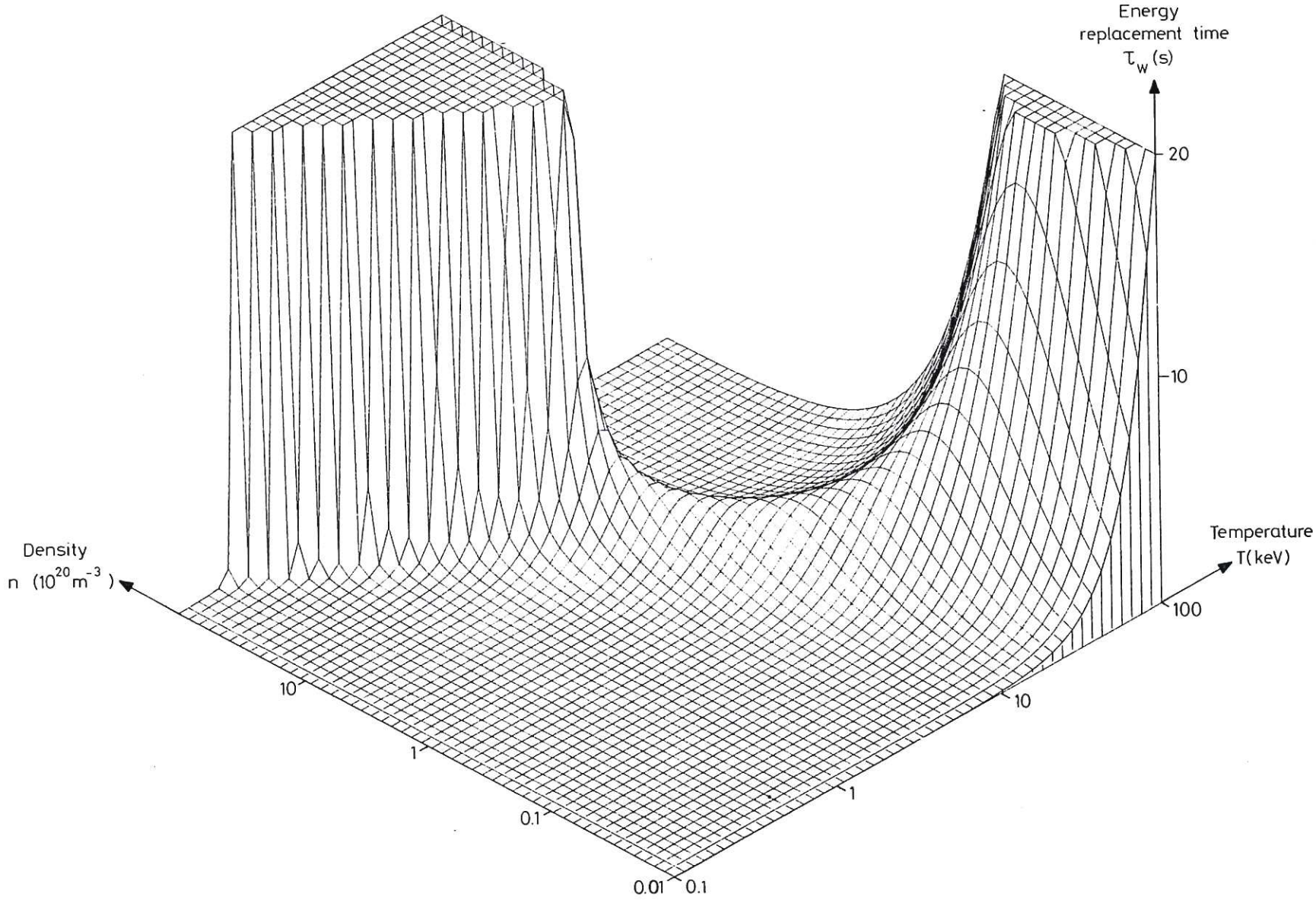

Fig.2 Isometric projection of the surface τ_W (n,T) for the same parameters as in Fig.1.

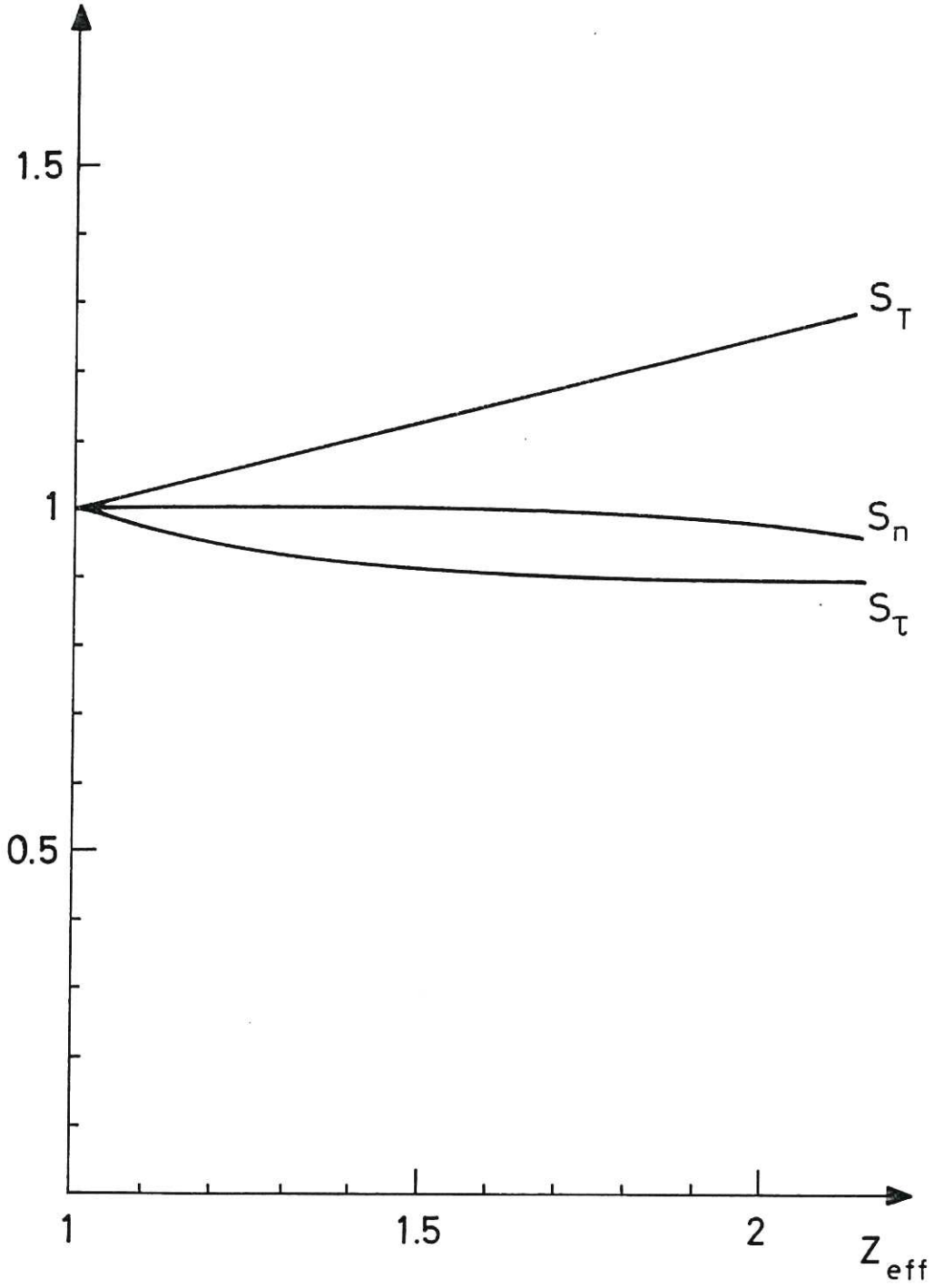

Fig.3 Dependence upon Z_{eff} of the saddle-point values n_*, T_*, τ_{W*} given by (14).

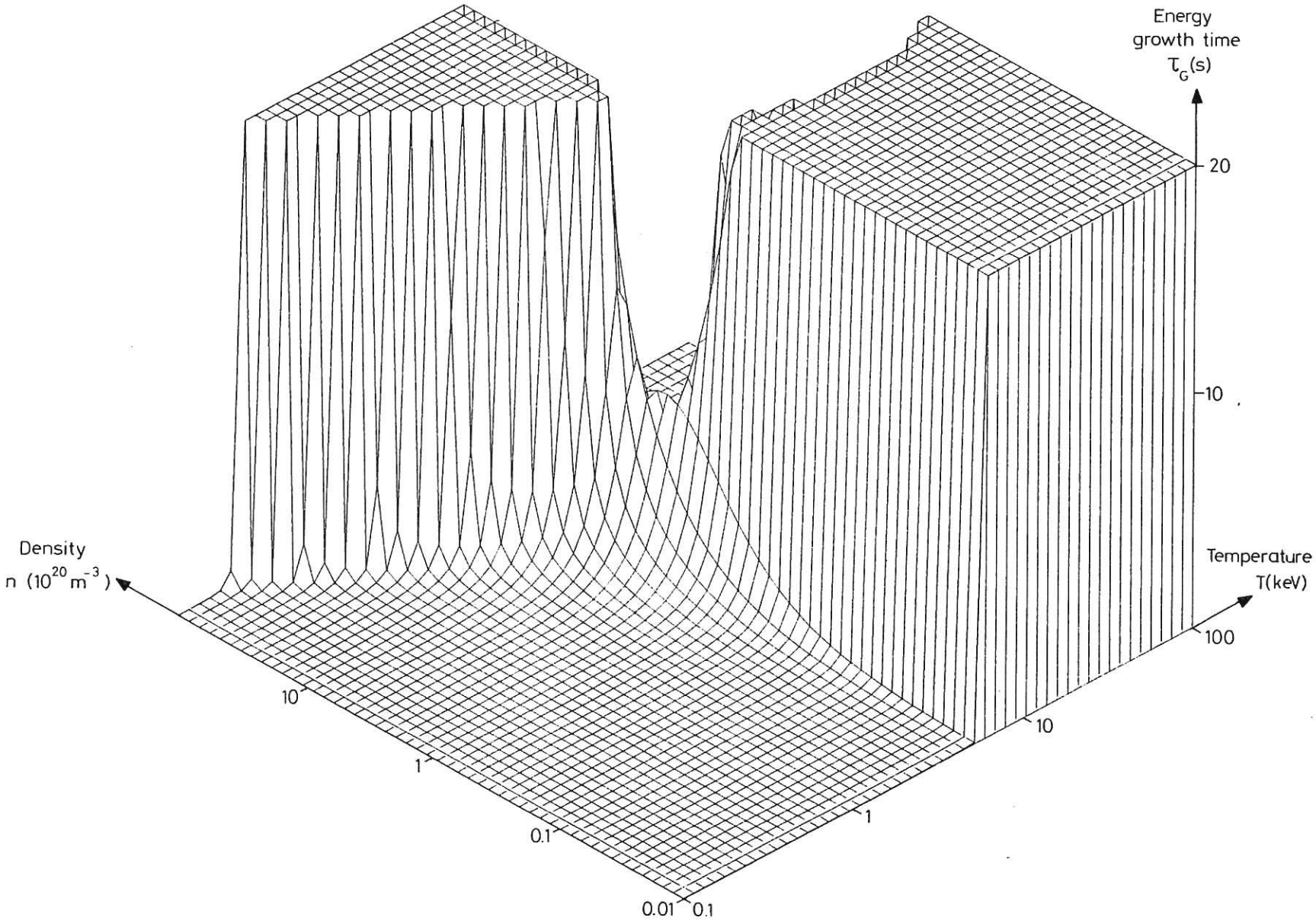

Fig.4 Isometric projection of the surface τ_G (n,T), energy growth time defined by (10). Same parameters as in Fig.1. τ_E given by the scaling law (8d).

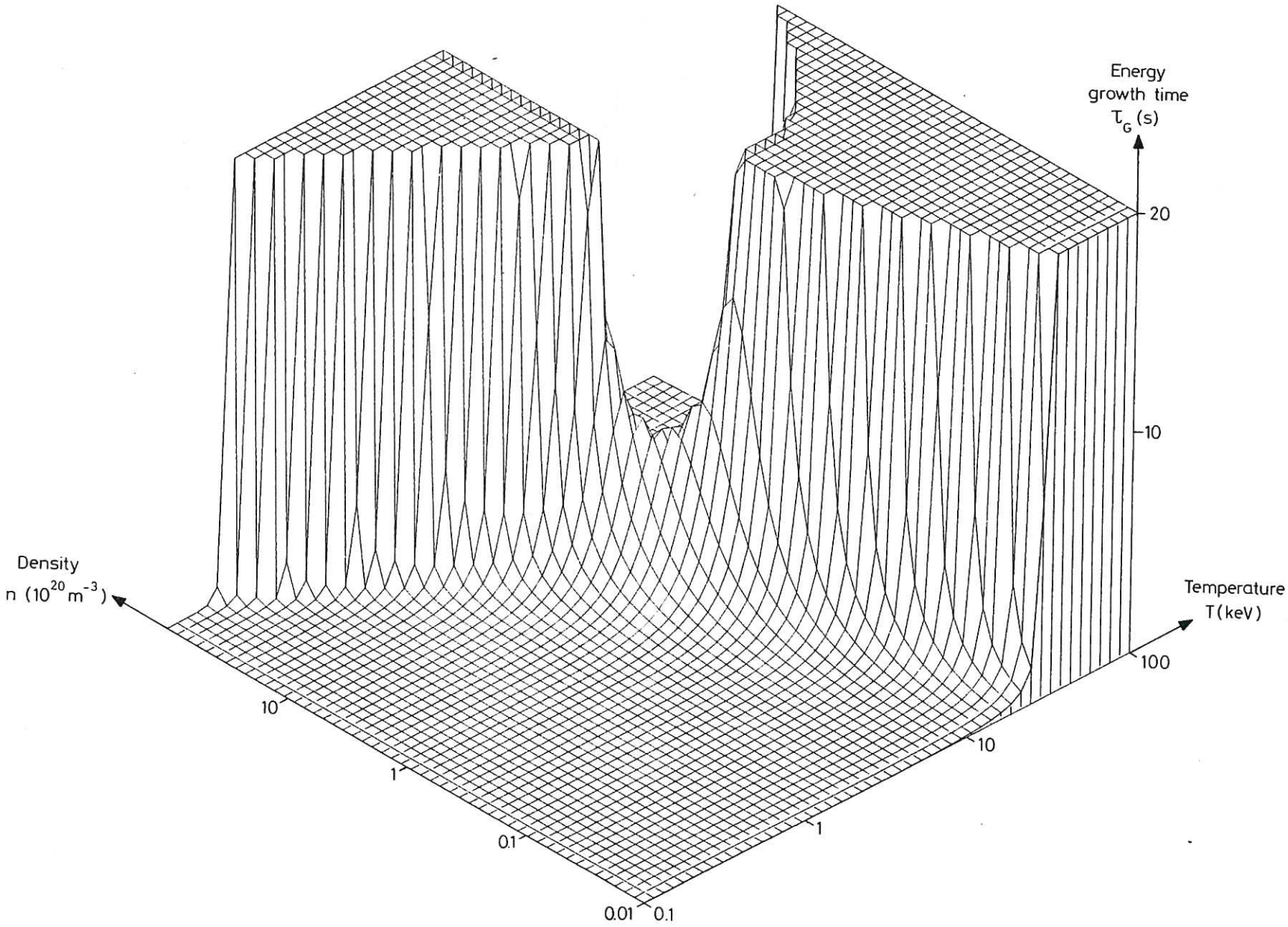

Fig.5 Isometric projection of the surface τ_G (n,T). Same parameters as in Fig.1. τ_E given by the scaling law (8b).

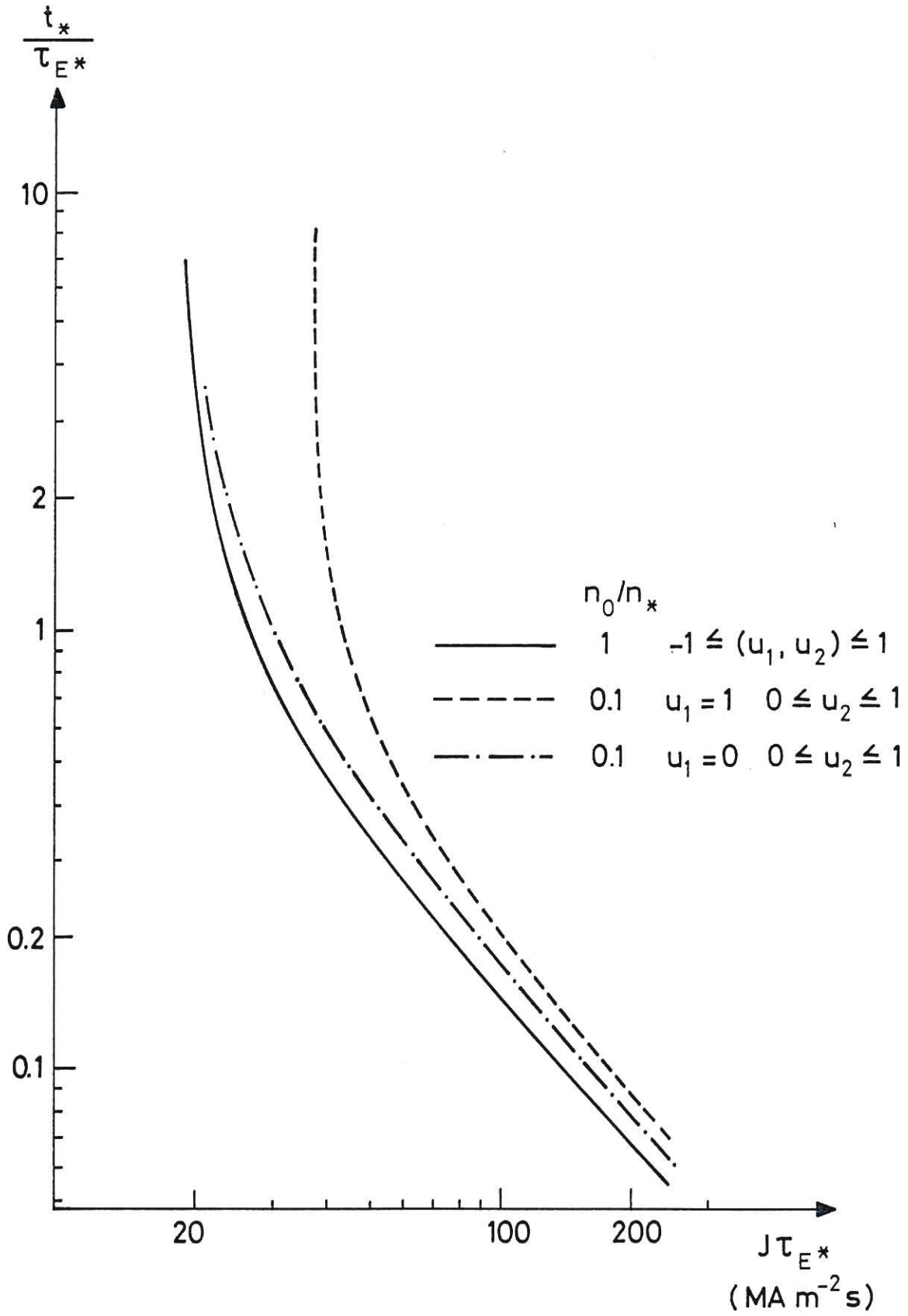

Fig.6 The ratio between ignition time t_* and the saddle-point value τ_{E*} against $J\tau_{E*}$. The three curves show that this ratio is insensitive to the choice of τ_E scaling (8) and (15).

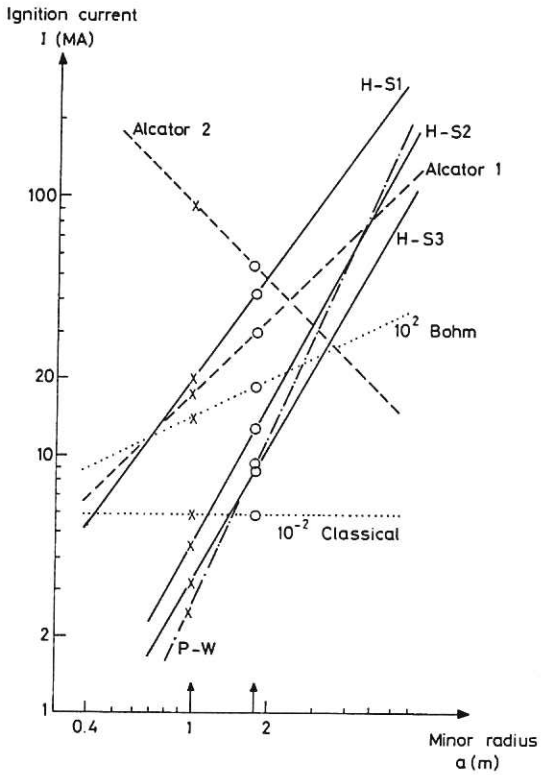

Fig.7 Current I required to reach ignition against minor radius a for the scaling laws (8).

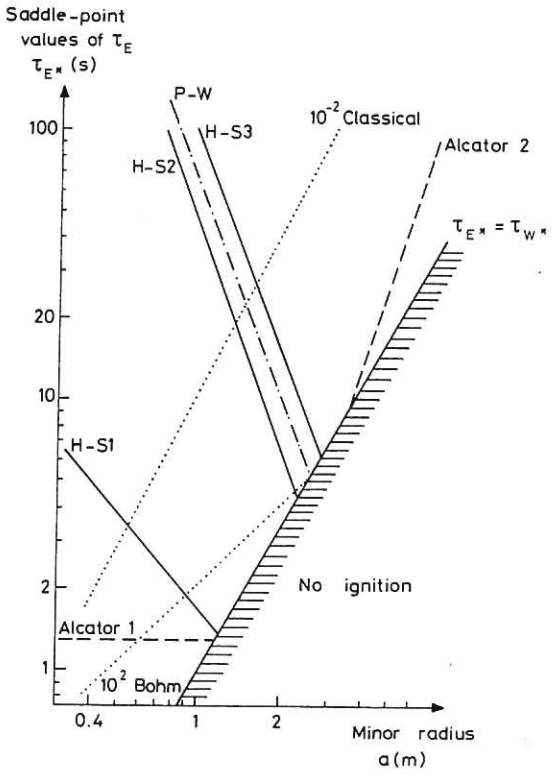

Fig.8 The minimum value $\tau_{E*} = \tau_{W*}$ needed for ignition at I = 20 MA and τ_{E*} predicted by (8) against minor radius a. The product aR_o is $250/\pi^2$ [m^2].